IOPscience iopscience.iop.org

Home Search Collections Journals About Contact us My IOPscience

Band-structure effects in the Hubbard chain

This article has been downloaded from IOPscience. Please scroll down to see the full text article.

1999 J. Phys.: Condens. Matter 11 4499

(http://iopscience.iop.org/0953-8984/11/23/304)

View the table of contents for this issue, or go to the journal homepage for more

Download details:
IP Address: 171.66.16.214
The article was downloaded on 15/05/2010 at 11:46

Please note that terms and conditions apply.

J. Phys.: Condens. Matter **11** (1999) 4499–4506. Printed in the UK PII: S0953-8984(99)00909-1

Band-structure effects in the Hubbard chain

Haranath Ghosh and Raimundo R dos Santos
Instituto de Física, Universidade Federal Fluminense, 24210-340 Niterói, Rio de Janeiro, Brazil

Received 12 January 1999, in final form 30 March 1999

Abstract. We present results of quantum Monte Carlo simulations for the one-dimensional Hubbard model with next-nearest-neighbour hopping (t_2). The appearance of double peaks in the spin and charge structure factors is identified with the doubling of ground states, each with its corresponding excitation modes. A quantitative phase diagram in the t_2–ρ (density) plane for fixed on-site coupling is obtained, and compared with weak-coupling renormalization group predictions. Four regions in this phase diagram are clearly identified: (i) singly peaked charge and spin structure factors; (ii) singly peaked ferromagnetic and charge fluctuations; (iii) singly peaked charge fluctuations and doubly peaked spin fluctuations; and (iv) doubly peaked spin and charge fluctuations.

The interplay between band-structure features and electronic correlations is responsible for a number of remarkable properties of low-dimensional fermionic systems. Indeed, for the Hubbard model in two dimensions, the concurrent van Hove singularity and nesting of the Fermi surface at half-filling give rise to an insulating antiferromagnetic (AFM) ground state for any finite on-site Coulomb repulsion U. As soon as the system is doped away from half-filling, it becomes a paramagnetic metal [1, 2], with weak short-ranged incommensurate spin–spin correlations [3, 4]. These concurrent effects can be separated by modifying the band structure through the inclusion of second-neighbour hopping, of magnitude t_2: as far as magnetic properties are concerned, a finite U, which increases with t_2, is now needed for the onset of antiferromagnetism at half-filling; away from half-filling, incommensurate peaks (again reflecting weak short-range correlations) appear in the magnetic structure factor [5–7]. It has also been suggested [8] that, as a result of second-neighbour hopping, the system at half-filling is a *non-magnetic metal* for small U, and undergoes a transition to a *metallic antiferromagnet* at a finite U_{c_1}; only at a larger U_{c_2} does it become an (AFM) insulator. Superconductivity from repulsive interactions also seems to arise as a result of second-neighbour hopping in the two-dimensional Hubbard model [7, 9, 10].

This intense activity on the two-dimensional Hubbard model has also triggered interest in the effects of second-neighbour hopping in one dimension, unveiling novel features. Firstly, the Lieb–Mattis theorem [11], which states that the ground state of the Hubbard model is a singlet, is no longer valid when second-neighbour hopping is active; this opens up the possibility of stabilizing a ferromagnetic ground state. In fact, for $U = \infty$, a low-*density* route to ferromagnetism (FM) has been proved to exist [12]; this should be contrasted with Nagaoka's low-*doping* (from half-filling) route [13]. For finite U, numerical data [14, 15] are consistent with FM in the ground state above a critical coupling, U_c, which typically increases with t_2 for fixed electronic density, ρ, below half-filling ($\rho < 1$); one expects $U_c \to \infty$ as $\rho \to 1$. Secondly, a weak-coupling renormalization group (WCRG) analysis [16] has

0953-8984/99/234499+08$19.50 © 1999 IOP Publishing Ltd

predicted the occurrence of many phases in the parameter space defined by electron density, strength of second-neighbour hopping, and on-site repulsion. In addition to the usual phases with spin- and charge-density waves (SDW and CDW), each with a single gapless excitation mode, others have been suggested to occur, such as a quasi-superconducting phase (i.e., strong superconducting correlations) and a gapped spin-liquid (dimer) phase; for the half-filled case, some of these predictions have been supported by density matrix renormalization group (DMRG) and quantum Monte Carlo (QMC) calculations [15, 17]. Furthermore, away from half-filling different spin- and charge-density-wave states have also been predicted [16], each characterized by *two* gapless excitations, the nature of which still awaits a full understanding; here we change slightly the notation of reference [16], and refer to these phases as SDWII and CDWII, respectively. One should note that it has hitherto been unclear how to reconcile the presence of FM with the SDWII and CDWII phases.

From the experimental side, the interest in one-dimensional systems has been revived by the unusual properties of ladder systems, such as $SrCu_2O_3$, and their possible relevance to high-temperature superconductors [18–20]. In particular, the zigzag structure of one-dimensional cuprates such as $SrCuO_2$ may be modelled by second-neighbour hopping terms [16]. Also, the recently discovered ladder superconductor [21] $Sr_{0.4}Ca_{13.6}Cu_{24}O_{41.84}$ (and related materials) has layers consisting of 1D chains alternating with layers of two-legged ladders. The triangular lattice (mimicked by t_2) is the key feature responsible for several effects such as the frustration of antiferromagnetic order, and asymmetry in the unperturbed density of states. Furthermore, these systems provide physical grounds for considering the regime $t_2 \simeq t$, which is customarily discarded.

Our purpose here is to take a closer look at the magnetic properties of the Hubbard chain with second-neighbour hopping. We will be particularly interested in elucidating the structure of the phases with more than one gapless excitation mode and how FM fits into this picture. A quantitative phase diagram will emerge from this analysis.

The Hubbard Hamiltonian is written as

$$\mathcal{H} = \sum_{\substack{i,j \\ \sigma}} t_{ij}(c^{\dagger}_{i\sigma}c_{j\sigma} + \text{h.c.}) + U\sum_{i}\left(n_{i\uparrow} - \frac{1}{2}\right)\left(n_{i\downarrow} - \frac{1}{2}\right) - \mu\sum_{i,\sigma} n_{i\sigma} \tag{1}$$

where the sums (i, j) run over sites of a chain with periodic boundary conditions, and

$$t_{ij} = \begin{cases} -t & \text{if } i \text{ and } j \text{ are nearest neighbours} \\ t_2 & \text{if } i \text{ and } j \text{ are next-nearest neighbours} \\ 0 & \text{otherwise.} \end{cases} \tag{2}$$

'h.c.' stands for Hermitian conjugate, $c^{\dagger}_{i\sigma}$ ($c_{i\sigma}$) creates (annihilates) a fermion at site i with spin σ, $U > 0$ is the repulsive on-site interaction, and μ is the chemical potential controlling the band filling. The sign of t is arbitrary since a gauge transformation $c_j \rightarrow \mathrm{e}^{\mathrm{i}\pi j}c_j$ can reverse it, so we set $t = 1$ without loss of generality, and measure all energies in units of t. When performed on this system, a particle–hole transformation [1] must be followed by the mapping $t_2 \rightarrow -t_2$ in order to recover the original Hamiltonian; that is, the parameter regime $(\rho > 1, t_2)$ is mapped onto $(\rho < 1, -t_2)$. We will therefore only discuss the behaviour for $t_2 > 0$, since that for $t_2 < 0$ can be inferred from the former. For $U = 0$, the dispersion $\epsilon(k)$ has one minimum at $k = 0$ for $t_2 < 0.25$, and two minima at finite k for $t_2 > 0.25$. Therefore, for small t_2, $\epsilon(k)$ does not differ qualitatively from the band structure for $t_2 = 0$, and there are two Fermi points for arbitrary electron density. On the other hand, for $t_2 > 0.25$ and sufficiently large densities, there are four Fermi points, namely $\pm k_{F_1}$ and $\pm k_{F_2}$, and the system can be mapped to a two-band model at weak coupling; the repulsive interaction U can cause

scattering among these Fermi points which may be the mechanism responsible for important modifications in the magnetic properties [16].

The system is studied by means of a grand-canonical quantum Monte Carlo (QMC) simulation; see references [1,22–24] for details. The imaginary time is discretized through the introduction of M 'time' slices separated by an interval $\Delta\tau$ such that $\beta \equiv \Delta\tau\, M$. The spin and charge degrees of freedom are probed by the magnetic and density structure factors:

$$S(q) = \frac{1}{N_s} \sum_{i,j=0}^{L-1} \langle m_i m_j \rangle \mathrm{e}^{\mathrm{i}q(r_i - r_j)} \tag{3}$$

$$C(q) = \frac{1}{N_s} \sum_{i,j=0}^{L-1} \langle n_i n_j \rangle \mathrm{e}^{\mathrm{i}q(r_i - r_j)} \tag{4}$$

with

$$m_i = n_{i\uparrow} - n_{i\downarrow} \tag{5}$$

and

$$n_i = n_{i\uparrow} + n_{i\downarrow}. \tag{6}$$

As this is a one-dimensional system, the relevant phase transitions only occur in the ground state. Accordingly, analytical studies of model (1) with $t_2 = 0$ at zero temperature [25, 26], as well as numerical studies for the t–J model at very low temperatures [27], indicate that the onset of quasi-long-range order is signalled by cusps or weak singularities in the above structure factors. However, when calculating averages such as those in equations (3) and (4) through QMC simulation, the so-called 'minus-sign problem' [23, 24] prevents us from reaching temperatures low enough for us to observe sharp features for all occupations and values of t_2. In the least favourable cases considered here, the lowest acceptable temperatures were those corresponding to $\langle \mathrm{sign} \rangle \sim 0.6$. Nonetheless, signatures of non-analytical behaviour can be seen even at temperatures that are not too low, as we now discuss.

Figure 1 shows the magnetic structure factor as a function of momentum transfer q, for $U = 2$; typical data are collected from over 10 000 MC sweeps through the lattice. Results for $\rho = 0.25$ and $t_2 = 0.15$ are shown in figure 1(a), for three different pairs of inverse temperature and system size $(\beta, N_s) = (7, 64)$, $(14, 40)$, and $(30, 40)$. The broad maximum at $\beta = 7$ signals the presence of a single dominant SDW, since it sharpens as the temperature is lowered towards $\beta = 30$; the peak position, in this case, is continuously displaced. Since finite-size effects are minimal for the magnetic structure factor (see below), one can safely perform a simple extrapolation of these peak positions towards $\beta = \infty$: it yields $q^*_{\mathrm{SDW}} \simeq \pi\rho = \pi/4$. Figure 1(b) shows results for $t_2 = 0.3$. Firstly, the comparison of $S(q)$ for different system sizes, ranging from $N_s = 36$ to 128, at $\beta = 7$ shows that finite-size effects can be safely neglected; we have checked that this holds true quite generally. Secondly, a ferromagnetic peak (i.e., at $q = 0$) dominates the fluctuation spectrum, and it corresponds to the low-density route to ferromagnetism; this peak gets more pronounced as the temperature is lowered, but its position remains unchanged. We have examined other combinations of t_2 and ρ to check for coexistence of the FM peak with another one, but found nothing. Figure 1(c), for a quarter-filled band ($\rho = 0.5$) and $t_2 = 0.6$, shows another possible outcome: the fluctuation spectrum is now dominated by two peaks, one of which is at $q = \pi$; as expected, these peaks sharpen as the temperature is lowered. A double peak in the structure factor marks the two most slowly decaying contributions to the correlation function in real space. That is, the system can stabilize two different SDWs, each with its own gapless excitation mode. This can be understood by recalling [12] that in this regime the model can be mapped onto two Hubbard chains coupled

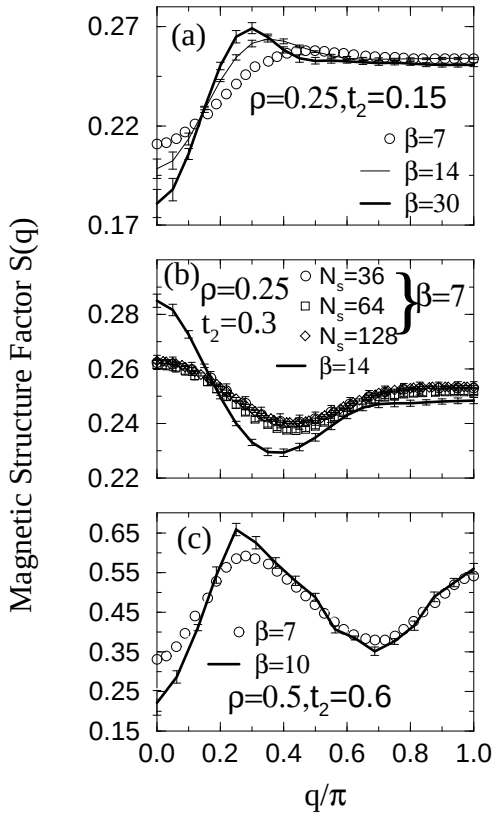

Figure 1. The magnetic structure factor (equation (3)) as a function of q for $U = 2$: (a) $\rho = 0.25$, $t_2 = 0.15$, and $\beta = 7$, 14, 30; (b) $\rho = 0.25$, $t_2 = 0.3$, and $\beta = 7$, 14; (c) $\rho = 0.5$, $t_2 = 0.6$, and $\beta = 7$, 10. All data for $\beta = 7$ are for $N_s = 64$, except in (b), where data for $N_s = 36$, 64, and 128 are compared; in (a) and (b) ((c)), the data for $\beta \geqslant 10$ are for $N_s = 40$ ($N_s = 32$).

through a ferromagnetic exchange coupling. Then, as far as the spin degrees of freedom are concerned, the system is in the SDWII phase, predicted through the WCRG analysis.

Figure 2 shows the charge structure factor, equation (4). For $\rho = 0.25$ and $t_2 = 0.15$ (figure 2(a)), $C(q)$ behaves similarly to in the $t_2 = 0$ case: a steady increase with q followed by a plateau. At zero temperature, a straight line with finite slope meets a horizontal line at q^*_{CDW}, thus marking the onset of the CDW instability. Though in this regime the plateau position shows a clear dependence on both ρ and t_2, extracting its precise functional form from finite-temperature data is in fact quite hard. Taking the $t_2 = 0$ case as a testing ground, successive estimates for $q^*(T)$—including the exact zero-temperature limit [25, 26], $q^*_{\mathrm{CDW}} = \pi\rho$—can be fitted to the function $q^*(T) \simeq 0.25\pi + 0.4T^{0.4}$, for $T < 0.125$. This form singles out a very sharp drop at temperatures so low ($T \lesssim 0.01$) that they lie way outside the range of our simulations. We are, therefore, only able to discuss the location of CDW instabilities in a qualitative fashion. As t_2 is increased to 0.38, keeping the density fixed at $\rho = 0.25$ (see figure 2(b)), a crossover to a different behaviour sets in. This new regime is characterized by the appearance of two peaks in the charge structure factor, as shown in figure 2(c); a similar crossover from a step-like cusp to a peak-like cusp has been observed previously in the context of the t–J model [27]. Similarly to the case for the spin degrees of freedom, this double-peak

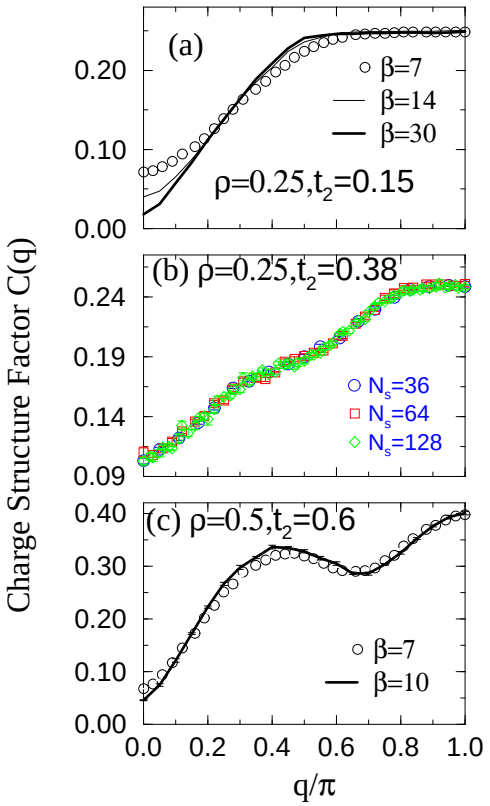

Figure 2. The charge structure factor (equation (4)); the notation is the same as for figure 1.

structure is identified with the CDWII phase, and hence with two excitation modes.

We extended the above analysis to many other values of $0 \leqslant t_2 \leqslant 0.6$ and $0 \leqslant \rho \leqslant 1$, identifying singly and doubly peaked regions. The ensuing phase diagram, on the t_2–ρ plane, is shown in figure 3, for fixed $U = 2.0$. The small-t_2 part is characterized by each structure factor displaying one singular point. For $|t_2| < 1/4$—where the free dispersion relation has a single minimum—the SDW peak positions are consistently located at $q^*_{\rm SDW} \simeq \pi\rho$. We therefore conclude that in this regime of 'small' nearest-neighbour hopping, the position of the SDW instability remains unshifted from its value at $t_2 = 0$, i.e. $q^* = 2k_F = \pi\rho$ [25, 26]. However, for occupations close to half-filling, one has $q^*_{\rm SDW} \simeq \pi$, as $|t_2|$ increases; this is a result of the hopping to every other site becoming more favourable. For $\rho \gtrsim 0.4$, and as t_2 increases, one enters an intermediate region in which the charge structure factor is still singly peaked, but the magnetic structure factor shows two peaks, one of which is always at $q = \pi$. At low densities, there is only one peak, corresponding to ferromagnetic fluctuations. As t_2 continues to increase, the charge structure factor develops a second peak; interestingly, the position of this second peak is almost independent of ρ and t_2, in contrast to what happens for $S(q)$. Also, the FM eventually disappears, so for fixed $U = 2$, FM is only possible within a small low-density window in the t_2–ρ plane. We should also mention that the phase diagram for the electron-doped region does not show the same features as for the hole-doped region: within the range of t_2 displayed in figure 3, the structure factors are singly peaked, and $q^*_{\rm SDW} = \pi\rho$.

In reference [15] a low-U phase diagram has been proposed, based on WCRG theory; the

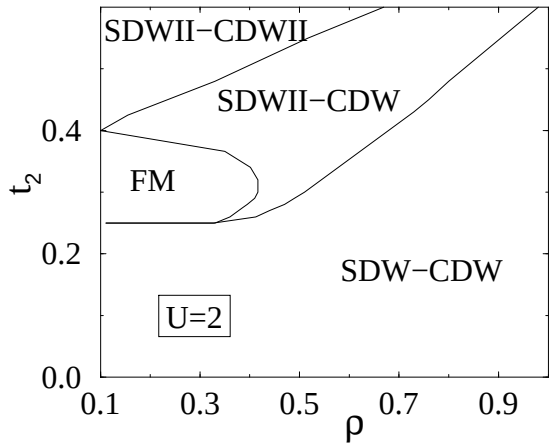

Figure 3. The phase diagram in the t_2–ρ plane, for $U = 2$. SDW–CDW stands for coexisting spin- and charge-density waves; SDWII–CDW stands for two predominant SDWs and one CDW; SDWII–CDWII stands for a SDW and a CDW, each with two predominant modes; FM stands for the ferromagnetic phase.

nature of the phases (i.e., whether they are gapped or gapless) has been checked by DMRG calculations of charge and spin gaps [15]. Though here we cover values of $|t_2|$ smaller than those in reference [15], a comparison of the predictions in the common range $0.6 \leqslant t_2 \leqslant 0$ is instructive. According to WCRG theory, the phase diagram consists mainly of two phases: (1) a usual Luttinger liquid (LL) phase, with a single gapless mode for each of the charge and spin excitations (SDW–CDW or C1S1, in the notation of reference [15]); and (2) a doped spin liquid, with gapped spin excitations and single gapless charge excitations (C1S0). Still according to WCRG theory, the LL phase is stable only while the Fermi 'surface' has two points (see figures 2, 18, and 19 of reference [15]); upon increasing $|t_2|$ very slightly and near half-filling, the system goes through two other phases, SDWII–CDWII and SDWII–CDW (or C2S2 and C1S2, respectively), before it reaches the doped spin-liquid regime. Our results agree with the prediction of a LL phase ending at a curve which follows very closely the one separating regions in which the Fermi 'surface' has either two or four points. On the other hand, the presence of gapped phases in the above range of t_2 has found only limited support from DMRG calculations [15]. Thus, it seems that in the absence of gapped phases, the SDWII–CDW and SDWII–CDWII phases occupy larger regions of the parameter space, as in figure 3. Another unsatisfactory aspect of the WCRG phase diagram is the absence of a FM phase: it emerges quite naturally from our analysis and within a range of parameters consistent with the predictions from Lanczos diagonalizations [15]. The discrepancies with respect to the WCRG phase diagram may be attributed to different sources, such as band-structure renormalization due to a finite U, or even to difficulties in solving the WCRG equations numerically [15].

Finally, we can fix both ρ and t_2, and study the structure factors with varying U; as mentioned before, the 'minus-sign problem' prevents us from examining the whole parameter space, but some conclusions may still be drawn from a limited set of data. Figure 4 shows the magnetic structure factor for $\rho = 0.25$, $t_2 = 0.15$, and for different values of the on-site coupling. For $U = 2$, this point lies outside the FM region in figure 3; accordingly, only a single peak is visible. As U increases, the structure factor flattens out, as shown in figure 4 for $U = 4$. Between $U = 5$ and 6, the FM peak appears, meaning that the SDW/FM transition boundary moves down as U increases; this is consistent with the notion of Fermi 'surface'

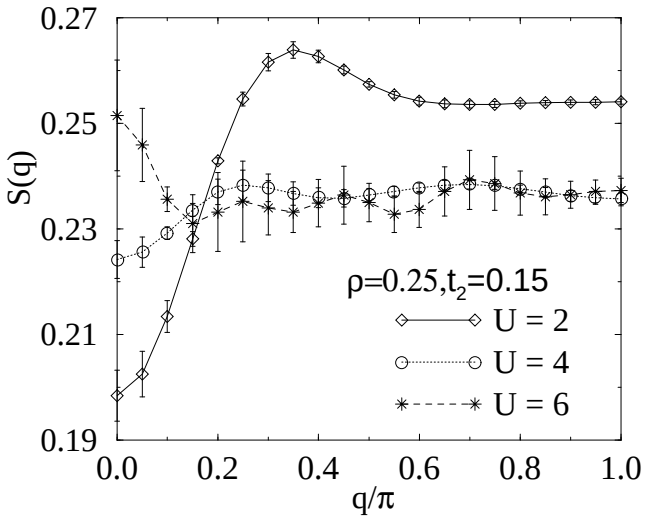

Figure 4. The magnetic structure factor (equation (3)) for a lattice with 40 sites at $\beta = 20$, $\rho = 0.25$, and $t_2 = 0.15$: data correspond to $U = 2$ (squares), $U = 4$ (stars), and $U = 6$ (circles).

becoming less appropriate for stronger couplings, so the boundary diverts considerably from that given by the appearance of four Fermi points in the non-interacting system. Thus, larger on-site couplings seem to cause a growth of the intermediate region, including both the FM and the SDWII–CDW phases, at the expense of the SDW–CDW phase.

In summary, we have carried out detailed Monte Carlo simulations of the one-dimensional Hubbard model with second-neighbour hopping, t_2. The charge and spin structure factors were calculated, and double peaks were identified with the two predominant density waves. We obtained a quantitative 'phase diagram' for fixed on-site coupling, $U = 2$. Below the four-Fermi-points region, the behaviour is qualitatively the same as if $t_2 = 0$, namely, dominated by single-peaked density waves; in particular, the SDW peak position, $\pi\rho$, is unaltered by the presence of second-neighbour hopping for all ρ, when $t_2 \lesssim 0.25$. Above this region, the major changes introduced by second-neighbour hopping are felt in two stages. First, there is an intermediate region in which only the spin modes are affected: at low densities, ferromagnetic fluctuations predominate, whereas at higher densities the SDWs are doubled. Then, only for larger values of t_2 are the charge modes affected by the appearance of a second CDW. As the on-site coupling increases, values of t_2 smaller than those predicted by WCRG theory [16] are sufficient to stabilize this intermediate phase.

Acknowledgments

Financial support from the Brazilian Agencies FINEP, CNPq, and CAPES is gratefully acknowledged; HNG also acknowledges financial support from FAPERJ.

References

[1] Hirsch J E 1985 *Phys. Rev.* B **31** 4403
Hirsch J E 1988 *Phys. Rev.* B **38** 12 023
[2] Hirsch J E and Tang S 1989 *Phys. Rev. Lett.* **62** 591

[3] Moreo A, Scalapino D J, Sugar R L, White S R and Bickers N E 1990 *Phys. Rev.* B **41** 2313
[4] For a list of more recent references, see, e.g.,
Dagotto E 1994 *Rev. Mod. Phys.* **66** 763
Kampf A P 1994 *Phys. Rep.* **249** 219
[5] Lin H-Q and Hirsch J E 1987 *Phys. Rev.* B **35** 3359
[6] Duffy D and Moreo A 1995 *Phys. Rev.* B **52** 15 607
[7] Veilleux A F, Daré A-M, Chen L, Vilk Y M and Tremblay A-M S 1995 *Phys. Rev.* B **52** 16 255
[8] Duffy D and Moreo A 1997 *Phys. Rev.* B **55** R676
[9] dos Santos R R 1989 *Phys. Rev.* B **39** 7259
[10] Husslein Th, Morgenstern I, Newns D M, Pattnaik P C, Singer J M and Matuttis H G 1996 *Phys. Rev.* B **54** 16 179
[11] Lieb E and Mattis D 1962 *Phys. Rev.* **125** 164
[12] Müller-Hartmann E 1995 *J. Low Temp. Phys.* **99** 349
[13] Nagaoka Y 1965 *Solid State Commun.* **3** 409
Nagaoka Y 1966 *Phys. Rev.* **147** 392
[14] Pieri P, Daul S, Baeriswyl D, Dzierzawa M and Fazekas P 1996 *Phys. Rev.* B **54** 9250
Daul S, Pieri P, Baeriswyl D, Dzierzawa M and Fazekas P 1997 *Physica* **230–232** 1021
Daul S and Noack R M 1997 *Z. Phys.* B **103** 293
[15] Daul S and Noack R M 1998 *Phys. Rev.* B **58** 2635
[16] Fabrizio M 1996 *Phys. Rev.* B **54** 10 054
[17] Kuroki K, Arita R and Aoki H 1997 *J. Phys. Soc. Japan* **66** 3371
[18] Azuma M, Hiroi Z, Takano M, Ishida K and Kitaoka Y 1994 *Phys. Rev. Lett.* **73** 3463
[19] Eccleston R S, Barnes T, Brody J and Johnson J W 1994 *Phys. Rev. Lett.* **73** 2626
[20] Dagotto E and Rice T M 1996 *Science* **271** 618
[21] Uehara M, Nagata T, Akimitsu J, Takahashi H, Môri N and Kinoshita K 1996 *J. Phys. Soc. Japan* **65** 2764
[22] Blankenbecler R, Scalapino D J and Sugar R L 1981 *Phys. Rev.* D **24** 2278
[23] Loh E Y Jr and Gubernatis J E 1992 *Electronic Phase Transitions* ed W Hanke and Yu V Kopaev (Amsterdam: Elsevier)
[24] von der Linden W 1992 *Phys. Rep.* **220** 53
[25] Ogata M and Shiba H 1990 *Phys. Rev.* B **41** 2326
[26] Frahm H and Korepin V E 1990 *Phys. Rev.* B **42** 10 553
[27] Assaad F F and Würtz D 1991 *Phys. Rev.* B **44** 2681